T · H · E
OHIO
STATE
UNIVERSITY

The Ogive as a RCS Compact Range Standard

A. Dominek and T. Nguyen

The Ohio State University
ElectroScience Laboratory
Department of Electrical Engineering
Columbus, Ohio 43212

Technical Report 719493-3
Grant No. NSG 1613
January 1989

National Aeronautics and Space Administration
Langley Research Center
Hampton, VA 22217

NOTICES

Contents

PRECEDING PAGE BLANK NOT FILMED

List of Figures

Chapter 1

Introduction

The performance of a compact range is dependent upon a variety of factors. However, once they have been optimized, the facility must be validated. One approach is to measure objects whose scattered fields are accurately known, such as perfectly conducting spheres and disks. These canoncial structures have scattered field solutions based upon eigenfunction solutions but the sphere is more often used since its solution is easier to calculate and, more importantly, its scattered field is more sensitive to illumination from other angles. It is this sensitivity which important since the compact range ideally generates plane wave illumination in the test zone.

The sphere is a good standard reference target but it does not provide a large dynamic range in its scattered field since it is dominated by a reflected field. Another standard target [1] is an ogive which provides excellent dynamic range but it has been inconvenient to use since its exact solution can not be generated by an eigenfunction solution. The most direct approach to calculate its exact scattered field is through a method of moments solution. This has been done for two different ogives. This report briefly describes the dominant scattering mechanisms for the ogive and presents calculated backscattered patterns which are compared with measured results for two ogives.

Chapter 2

Scattering Mechanisms

The high frequency representation of backscattered fields can be divided into three regions [2] which are shown in Figure 2.1. The angular sector between 0^o and 90^o is divided into these regions based upon the visibility of the rear tip and the presence of a specular field. Region I is between 0^o and α where α is the half tip angle of the ogive. Region II is between α and $90^o - \alpha$. Region III is between $90^o - \alpha$ and 90^o. Region I has scattering due to direct front tip illumination, creeping wave illumination of the rear tip and tip to tip interactions involving various creeping wave paths. Region II has scattering due to direct front and rear tip illumination and tip to tip interaction through creeping waves. Regions II and III have similar scattering mechanisms but with the presence of a dominant specular scattering mechanism in Region III.

The backscattered field from an ogive can be decomposed into two polarization planes; i.e. the E- and H-planes. The incidence plane is formed by the incident ray and the two tips of the ogive. The E- and H-plane patterns have the electric field vector parallel and normal to the incidence plane, respectively. The patterns for both planes are similar in Region III due to the polarization independence of the specular field. The major difference occurs due to the boundary condition of the electric field that has to be satisfied in Region I for the two polarization planes. The E-plane scattered field supports a significant creeping wave (normal electric field to the surface) in Region I which scatters back due to the rear tip. To provide a continuous field value in Region II, the rear tip has to scatter strongly as)ecomes directly illuminated. The H-plane scattered field from the reat does not require a large value as it becomes directly illuminated since re is not a significant creeping wave (parallel electric field to the surface) minating the rear tip in Region I.

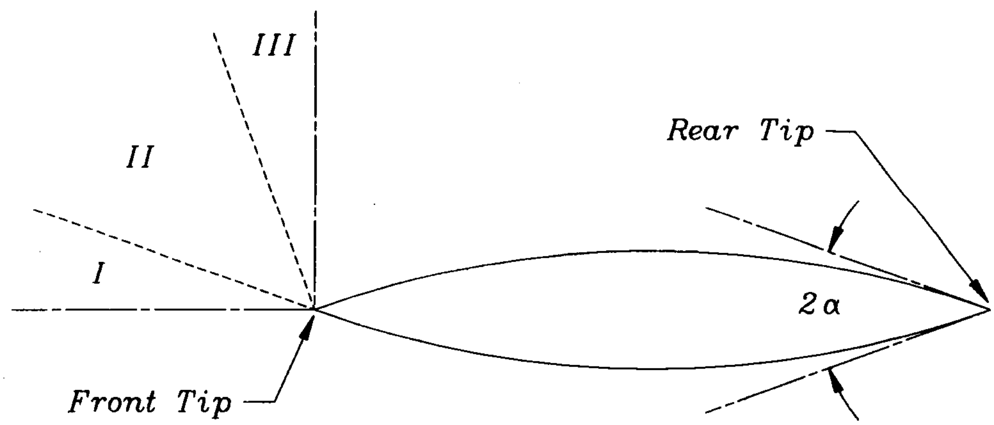

Figure 2.1: Dominant scattering mechanisms for a perfectly conducting ogive.

Chapter 3

Calculations

The E- and H-plane RCS patterns for two perfectly conducting ogives were calculated using a body of revolution moment method code [3]. The calculations were performed on a Cray computer [4] to facilitate the computations. The computation involved the solution of many unkowns due to the large electrical size of the ogives. The sampling length of each segment was no greater than one tenth of a wavelength long. The dimensions for the ogives, identified as A and B, are in Table 3.1. Figures 3.1 and 3.2 illustrate the E- and H-plane RCS patterns for the 9.546" long ogive at 10 GHz, respectively. Figures 3.3 and 3.4 illustrate the E- and H-plane RCS patterns for the 36" long ogive at 4 GHz, respectively. Figures 3.5 and 3.6 illustrate the E- and H-plane RCS patterns for the 36" long ogive at 10 GHz, respectively. All cross section values are calibrated in dBsm.

Table 3.1: Physical dimensions for the ogives

Ogive	A	B
Tip to tip length (in)	9.546	36
Radius (in)	14	69.548
Half tip angle (D)	20	15
Girth Diameter (in)	1.683	4.739

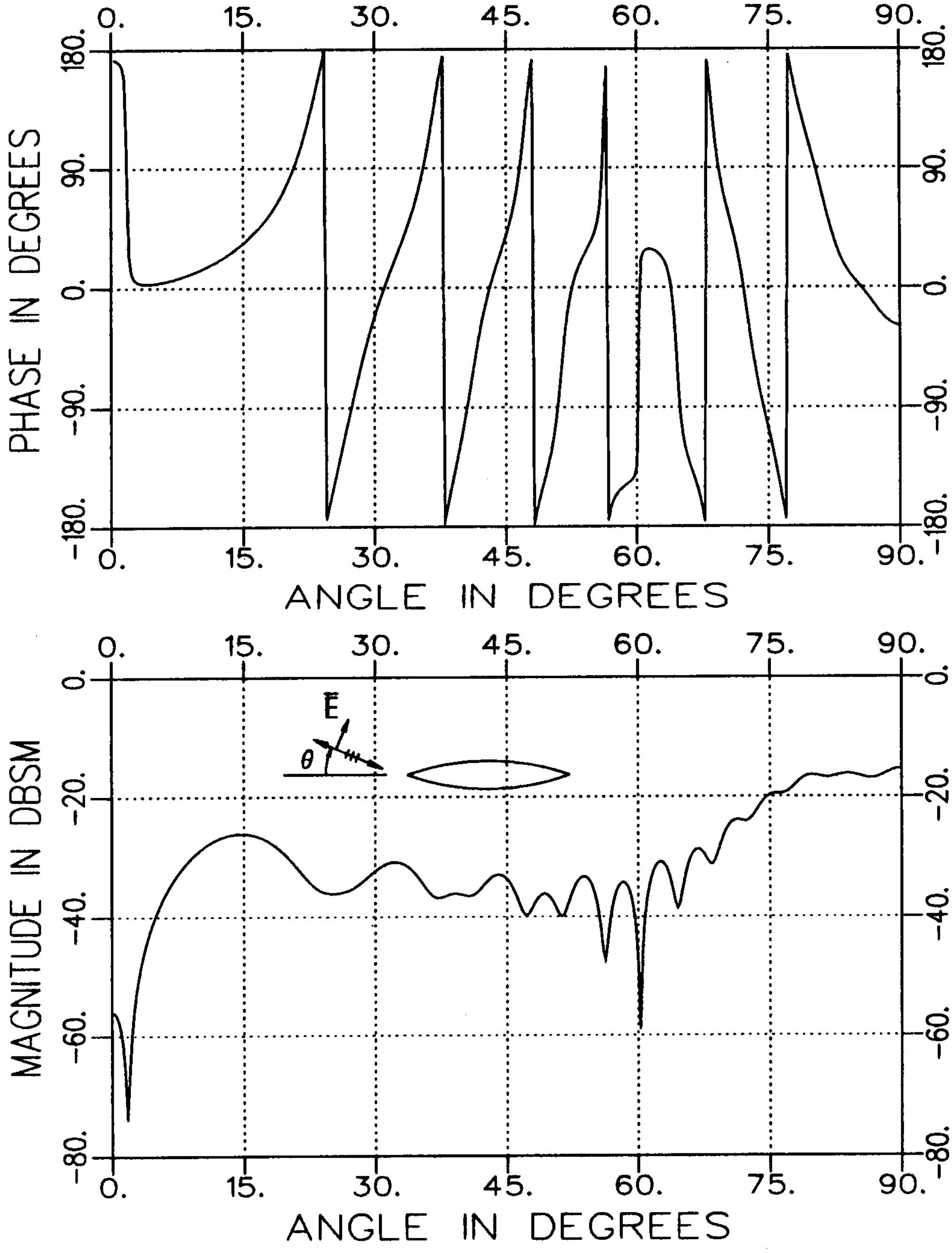

Figure 3.1: E-plane RCS pattern calculation for the 9.546" long ogive at 10 GHz.

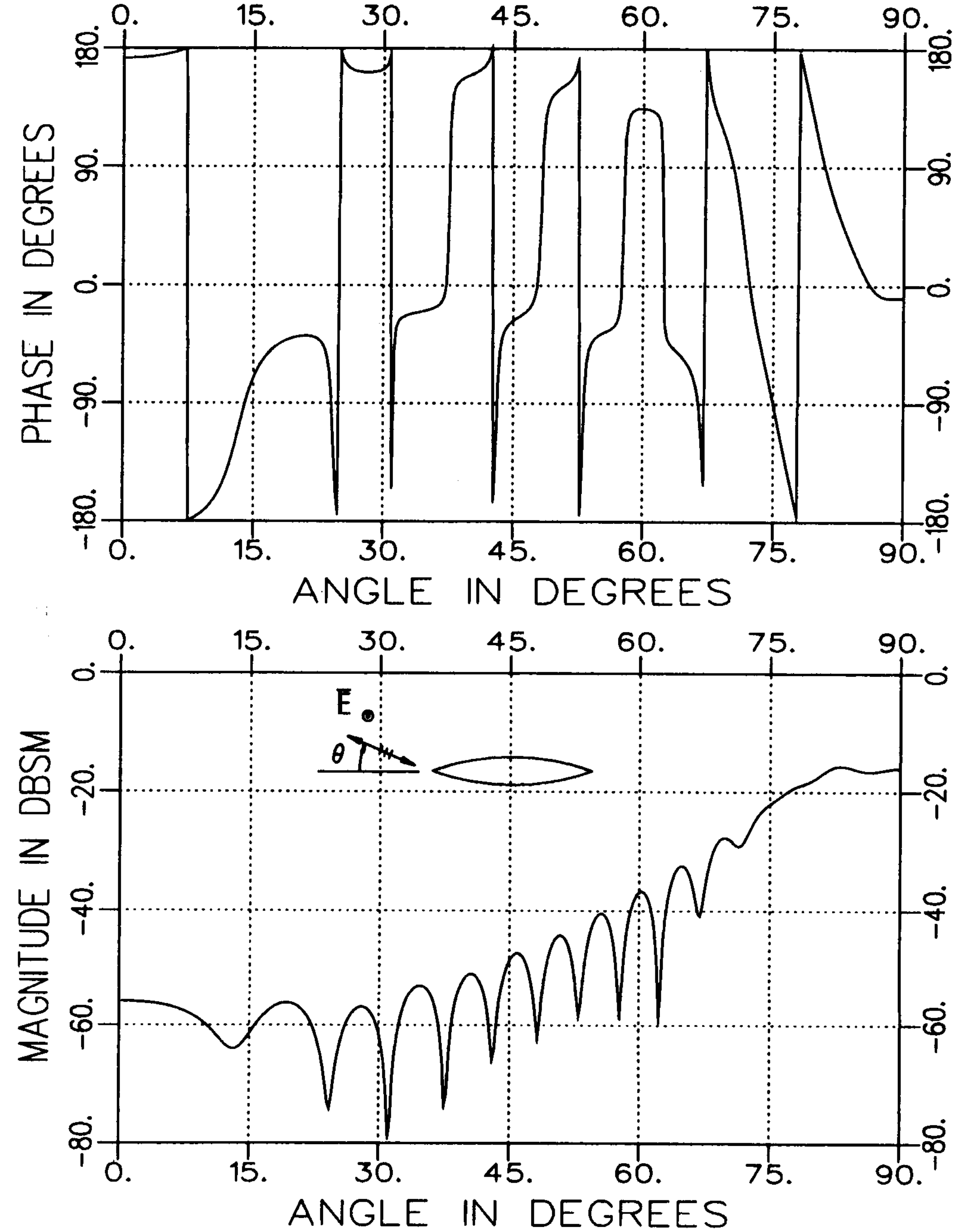

Figure 3.2: H-plane RCS pattern calculation for the 9.546" long ogive at 10 GHz.

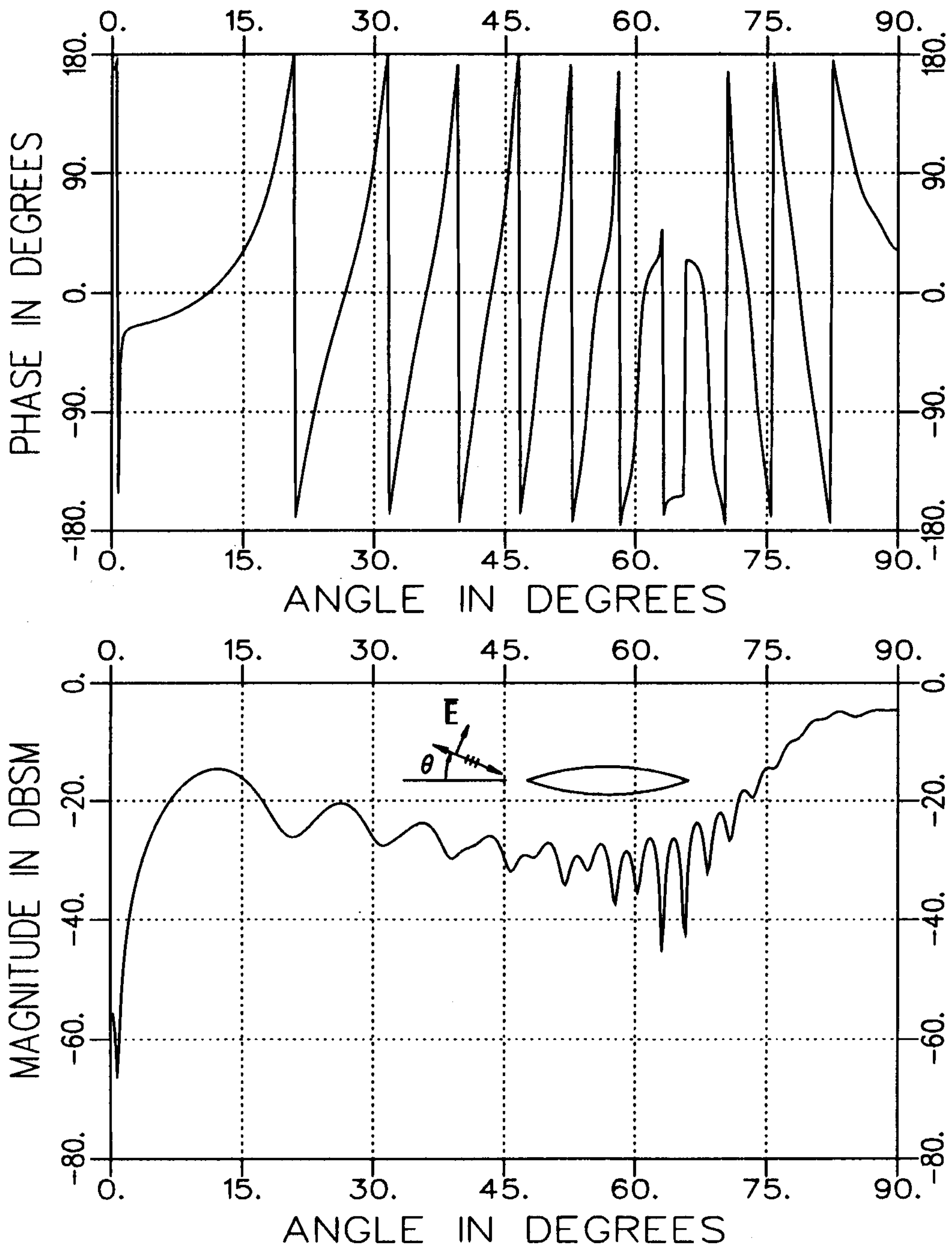

Figure 3.3: E-plane RCS pattern calculation for the 36" long ogive at 4 GHz.

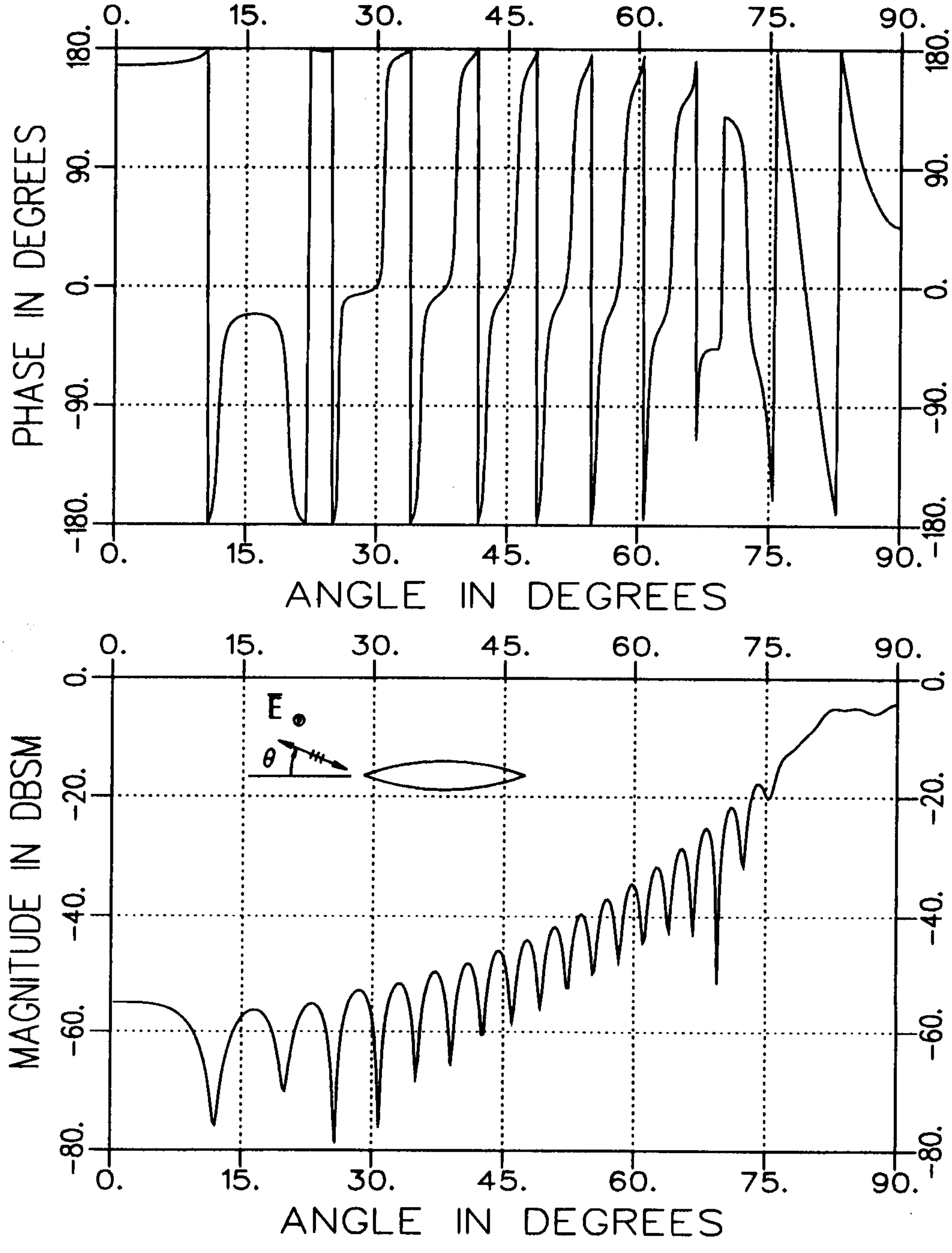

Figure 3.4: H-plane RCS pattern calculation for the 36" long ogive at 4 GHz.

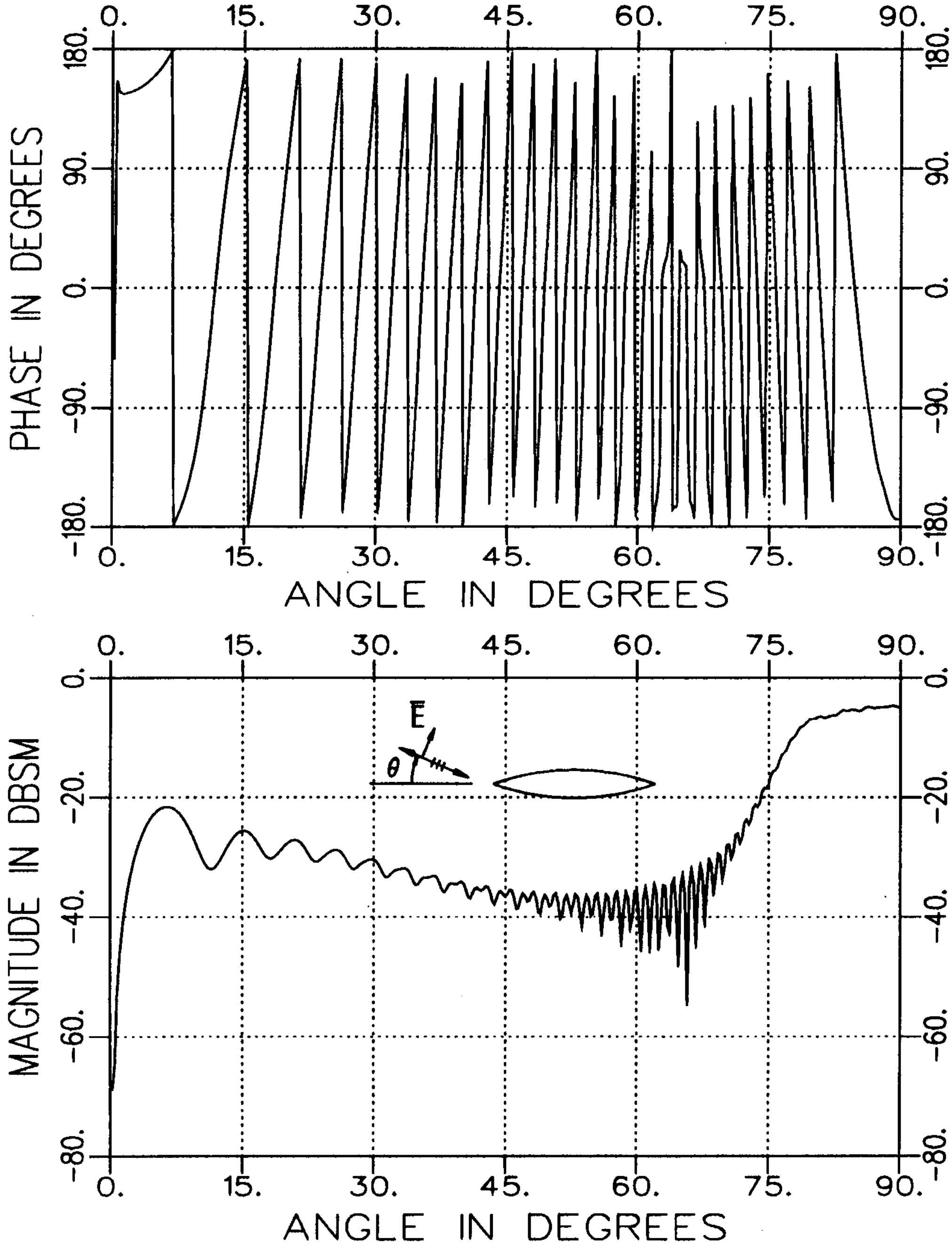

Figure 3.5: E-plane RCS pattern calculation for the 36" long ogive at 10 GHz.

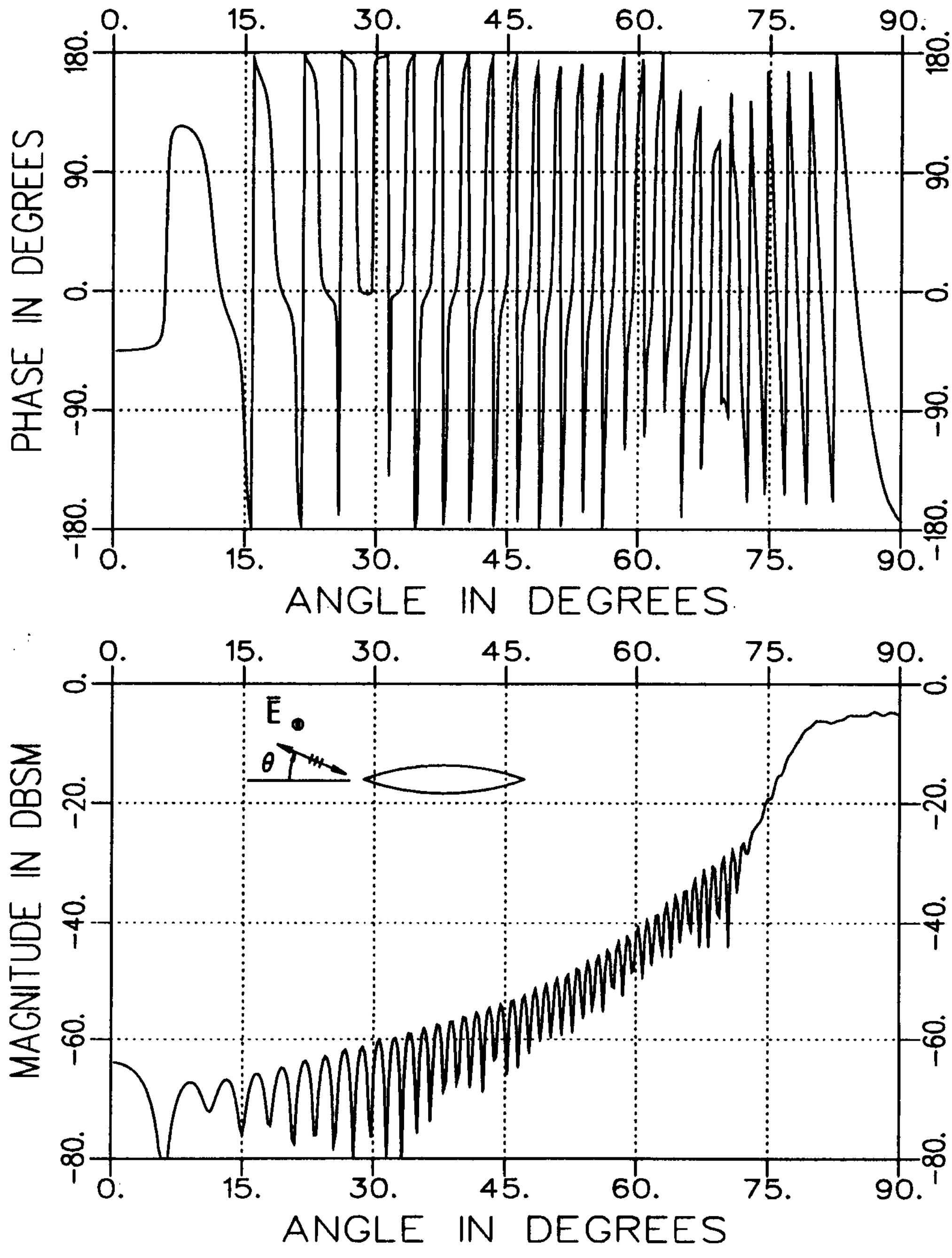

Figure 3.6: H-plane RCS pattern calculation for the 36" long ogive at 10 GHz.

Chapter 4

Measurements

RCS pattern measurements were performed at the ElectroScience Laboratory compact range for both the 36" and 9.546" long ogives. The 36" long ogive was provided by NASA Langley Research Center and was constructed from a silver painted, fiberglas covered foam ogive with metal tips. The 9.546" long ogive was constructed from a piece of solid aluminum. Each measurement consisted of a vector background subtraction, where the measured returns with and without a target present in the range are subtracted. The ogives were positioned on a 2.75" diameter styrofoam column which connected to a treated low cross section metal ogival pedestal. The following figures illustrate the measured response as a solid line and the calculated one by a dashed line with all values calibrated in dBsm. Figure 4.1 illustrates the E-plane pattern comparison for the 9.546" long ogive. Figures 4.2 and 4.3 illustrate the E-plane pattern comparison for the 36" long ogive at 4 and 10 GHz, respectively. Figures 4.4 and 4.5 illustrate the H-plane pattern comparison for the 36" long ogive at 4 and 10 GHz, respectively. As can be seen, the E-plane patterns generally have good agreement between calculated and measured responses. However, the H-plane pattern comparisons do not agree as well in the low level regions due to the mount contamination and model imperfections. This is confirmed with swept frequency measurements that have been transformed into the time domain to obtain down range scattering center mechanism identification. Figure 4.6 is an illustration of such a time domain signature for a 36" long ogive at axial incidence. Note the presence of error terms which are significant at low RCS levels.

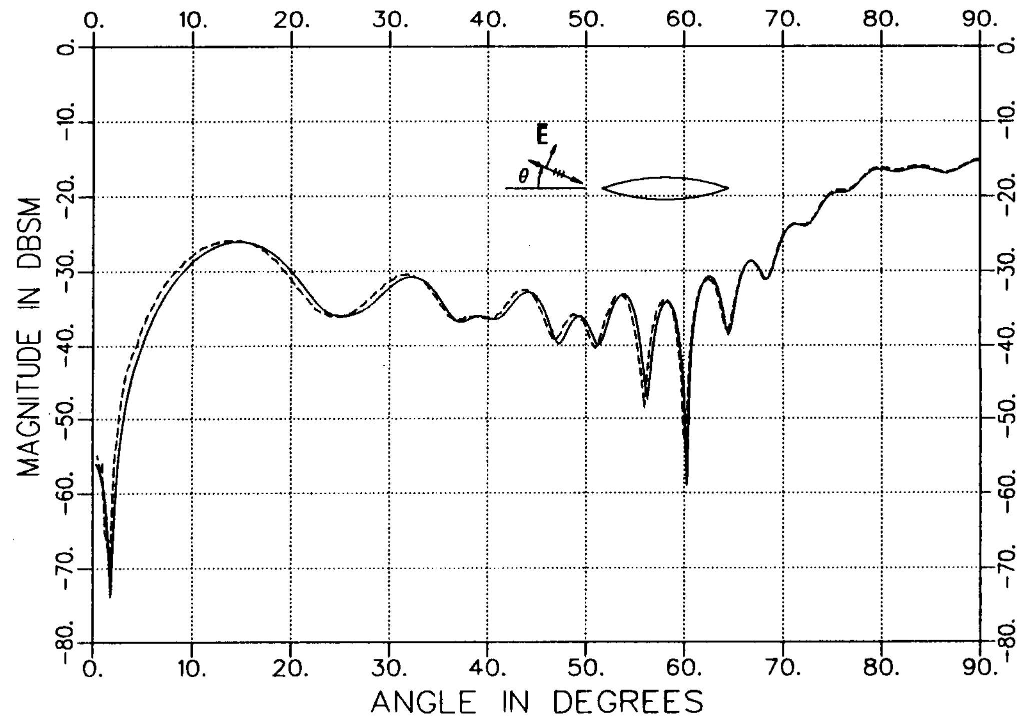

Figure 4.1: E-plane RCS pattern comparison for the 9.546" long ogive at 10 GHz. Solid-measured, Dashed-calculated

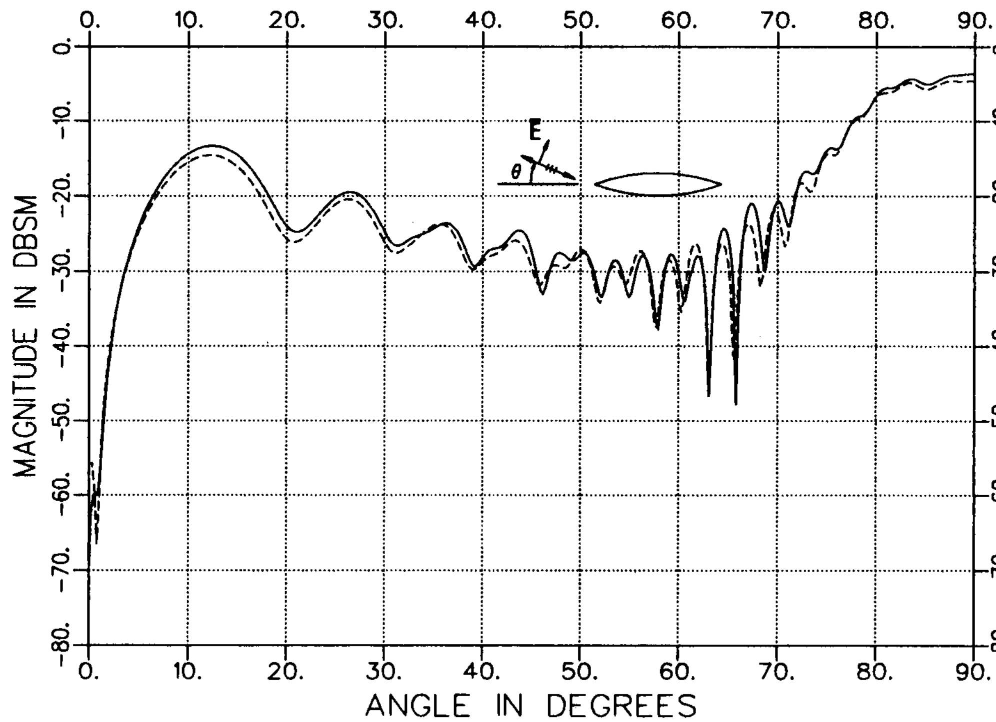

Figure 4.2: E-plane RCS pattern comparison for the 36" long ogive at 4 GHz. Solid-measured, Dashed-calculated

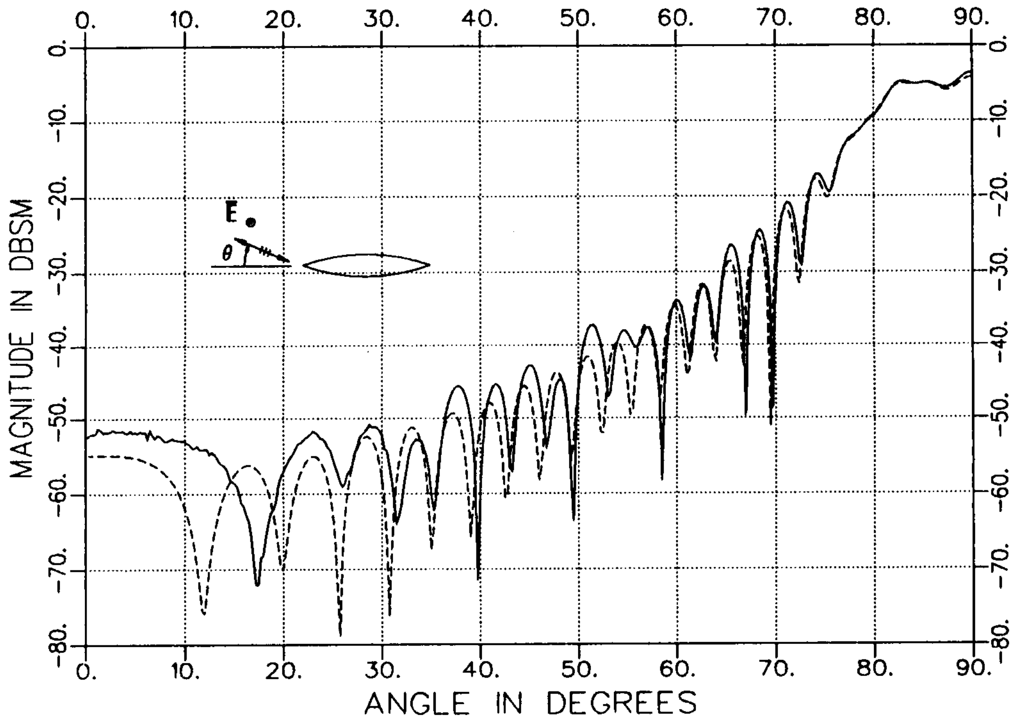

Figure 4.3: H-plane RCS pattern comparison for the 36" long ogive at 4 GHz. Solid-measured, Dashed-calculated

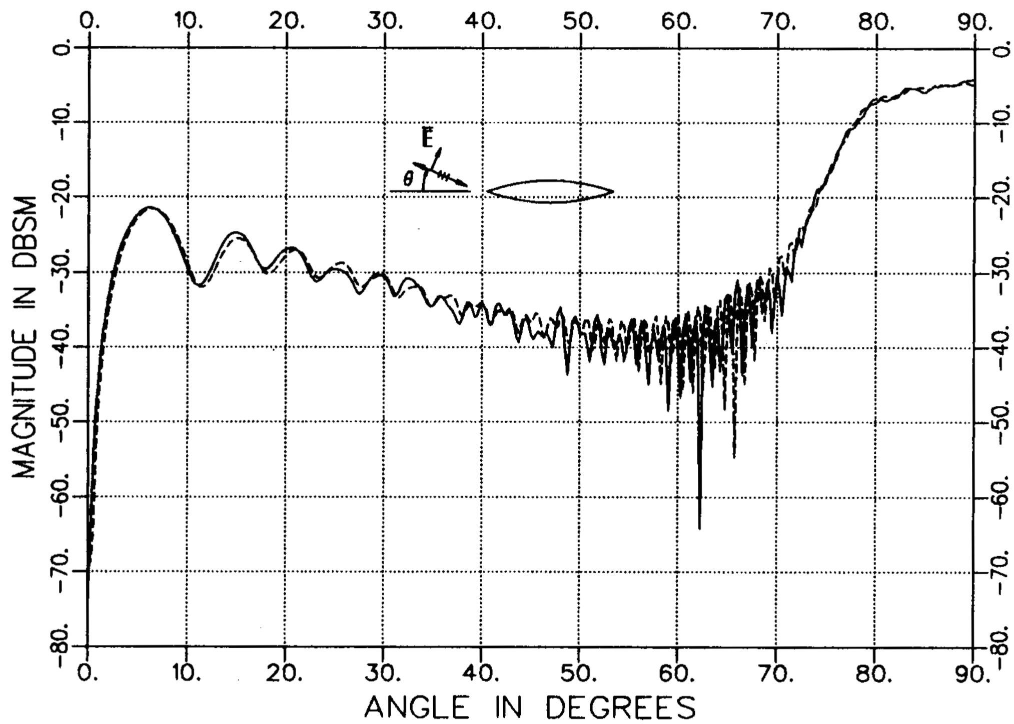

Figure 4.4: E-plane RCS pattern comparison for the 36" long ogive at 10 GHz. Solid-measured, Dashed-calculated

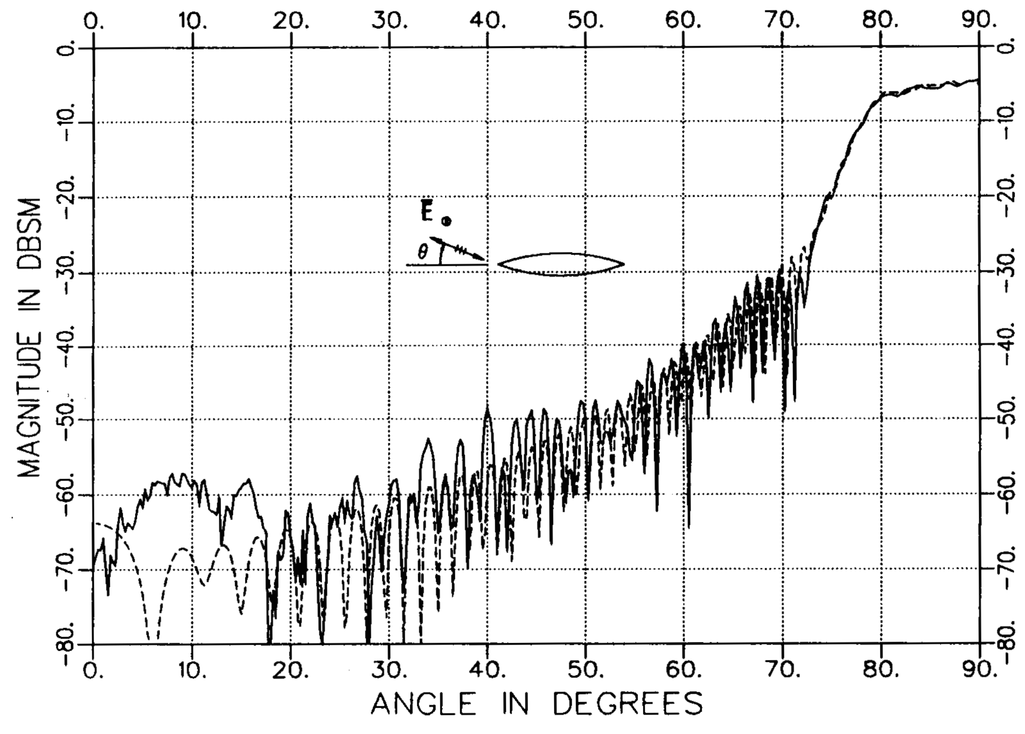

Figure 4.5: H-plane RCS pattern comparison for the 36" long ogive at 10 GHz. Solid-measured, Dashed-calculated

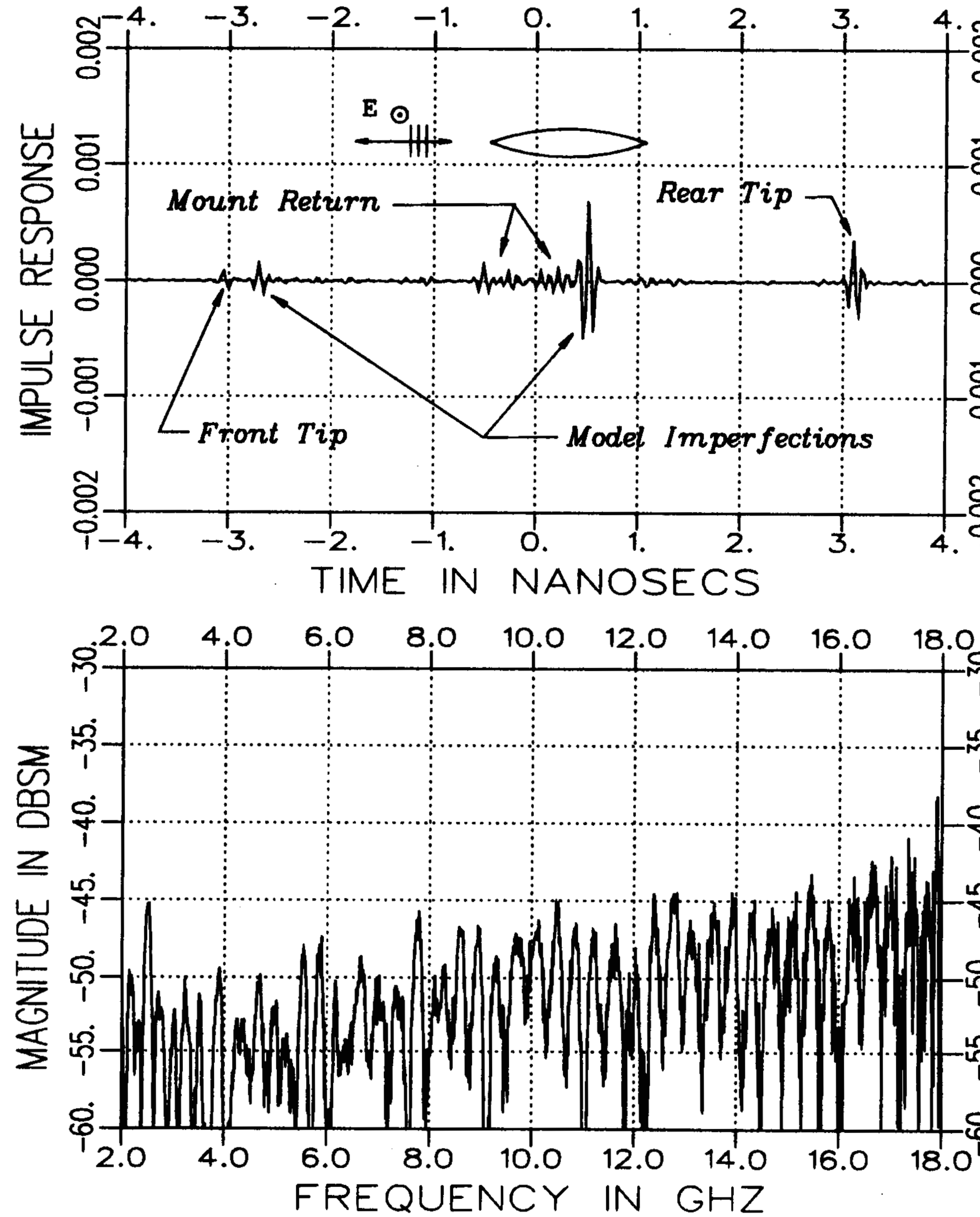

Figure 4.6: RCS spectrum and transient signature for the 36" long ogive at axial incidence demonstrating the presence of error terms.

Chapter 5

Conclusions

The measured H-plane scattered field pattern of an ogive is an excellent test of a compact range due to its large dynamic range. It has a very broad low level response (approximately -60dBsm) as well as a high level specular return. The ability to obtain patterns of the quality shown here is not only dependent upon the reflector system and instrumentation radar but also on target mounting techniques and target fabrication ability which are important aspects that are sometimes overlooked.

Bibliography

[1] L. Peters, Jr., W.D. Burnside and A. Dominek, "Some Useful RCS Test Bodies," Antenna Measurements Techniques Association Conference, Melbourne, FL, September, 1985.

[2] H. Shamansky, Ph.D Dissertation in preparation, Department of Electrical Engineering, The Ohio State University, Columbus, OH.

[3] A.J. Terzuoli, Jr., C.W. Chuang, and L. Peters, Jr. "An Integral Equation Approach To Obtain The Significant Parameters Of Dihedral Corrugated Horns," Report No. 3821-2, ElectroScience Laboratory; Prepared under Grant GK-404809 for the National Science Foundation, July 1976.

[4] Ohio Supercomputer Center, 1224 Kinnear Road, Columbus, OH.

50272-101

REPORT DOCUMENTATION PAGE	1. REPORT NO.	2.	3. Recipient's Accession No.

4. Title and Subtitle THE OGIVE AS A RCS COMPACT RANGE STANDARD	5. Report Date January 1989 6.
7. Author(s) A. Dominek and T. Nguyen	8. Performing Org. Rept. No. 719493-3
9. Performing Organisation Name and Address The Ohio State University ElectroScience Laboratory 1320 Kinnear Road Columbus, OH 43212	10. Project/Task/Work Unit No. 11. Contract(C) or Grant(G) No. (C) (G) NSG 1613
12. Sponsoring Organisation Name and Address National Aeronautics and Space Administration Langley Research Center Hampton, VA 22217	13. Report Type/Period Covered Technical 14.

15. Supplementary Notes

16. Abstract (Limit: 200 words)

E- and *H*-plane RCS patterns at 4 and 10 GHz are provided (based upon moment method calculations) for a perfectly conducting ogive to be used as a compact range verification standard. The dimensions of the ogive are 36″ and 9.546″ long with half tip angles of 15° and 20°, respectively. Comparison between the calculations and measurements are also provided.

17. Document Analysis a. Descriptors

b. Identifiers/Open-Ended Terms

c. COSATI Field/Group

18. Availabilty Statement	19. Security Class (This Report) Unclassified	21. No. of Pages 21
	20. Security Class (This Page) Unclassified	22. Price

(See ANSI-Z39.18) *See Instructions on Reverse* OPTIONAL FORM 272 (4-77)
Department of Commerce